Karlsruhe Institute of Technology

# Stress-dependent vibration peaks in glass

- Literature results

K. Günter Schell, Claudia Bucharsky, Susanne Wagner, Theo Fett

KIT SCIENTIFIC WORKING PAPERS **253**

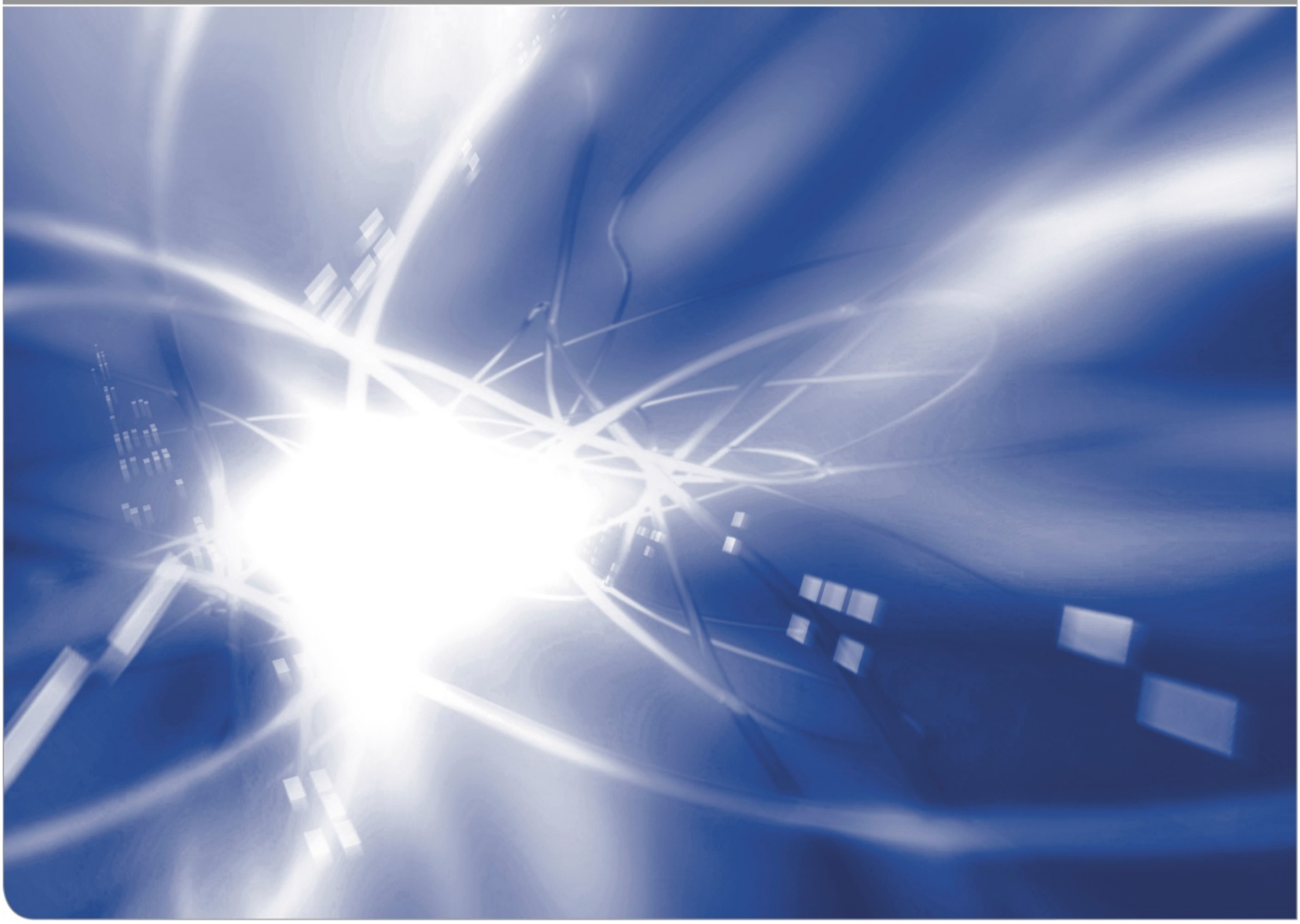

## Institute for Applied Materials

**Impressum**

Karlsruher Institut für Technologie (KIT)
www.kit.edu

This document is licensed under the Creative Commons Attribution – Share Alike 4.0 International License (CC BY-SA 4.0): https://creativecommons.org/licenses/by-sa/4.0/deed.en

2024

ISSN: 2194-1629

## Abstract

When glass is subjected to mechanical stress, it is found that the IR- and Raman lines are shifted relative to their position in the stress-free state. It is shown that for almost all lines a decrease in the wave number occurs under tensile stresses and an increase under compressive stresses.

When plotted against the maximum stress component, larger changes in wave number are generally observed in hydrostatic compression tests compared to tensile tests. When plotted against the hydrostatic stress component, the slopes under compression and tension are quite comparable.

We made a short *literature review* on experimental measurements. It can be seen that in the range of about 1060/cm to 1120/cm the influence of stress in both the tensile and compressive ranges is almost negligible.

The reason for this abnormal behavior will be investigated in a separate study.

# Contents

**1 Position of IR- and Raman-maxima under stresses** 1

1.1 Asymmetric stretching mode (AS) 1

1.2 Symmetric stretching mode (SS) 2

1.3 Peak position for Raman peaks below 700/cm 4

**2 Summary of results** 4

**3 Main conclusions** 6

**References** 7

# 1. Position of IR- and Raman-maxima under stresses

## 1.1 Asymmetric stretching mode (AS)

The influence of uniaxial tensile stresses on the peak position of IR- and Raman-lines that has been measured by Tallant et al. [1], is shown in Fig. 1 with the peak position in terms of the wavenumber. These Raman-data were obtained in tensile test and the results are introduced as the red squares.

Measurements of the IR-peak in 2-point bending tests were performed by Tomozawa et al. [2]. The results for as-received fibres are introduced by the red circles. After annealing and etching away a surface layer of about 1µm thickness, the measured data are shown by the black circles. The blue squares were obtained from the Raman spectra shown in Fig. 2 of the paper by Hemley et al. [3].

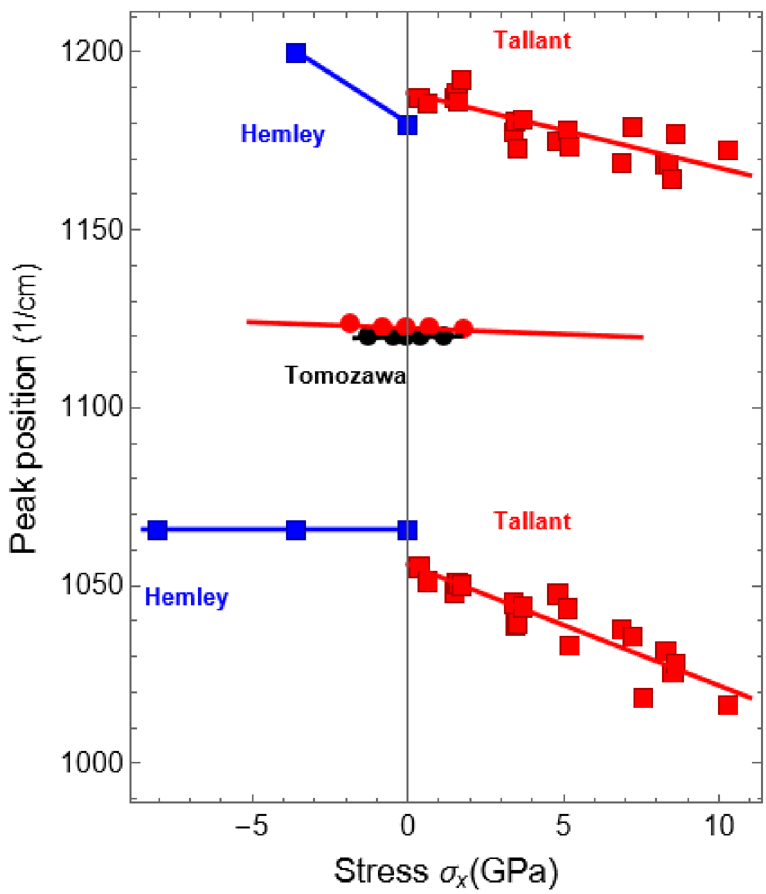


**Fig. 1** Measurements of Raman peak in the region of “asymmetric stretching (AS)” by Tallant et al. [1] on silica by uniaxial tensile tests (red squares). Data of IR-peak from bending tests by Tomozawa et al. [2] (red and black circles), evaluation of Raman curves by Hemley et al. [3] (blue squares).

The peak position (in the following abbreviated by $P$ in terms of 1/cm) for uniaxial tension $\sigma_x$ (in GPa) was found for the measurements by Tallant et al.[1]:

$$P = 1188 - 2.11\,\sigma_x \tag{1}$$

and

$$P = 1056 - 3.40\,\sigma_x \tag{2}$$

From the 2-point bending tests by Tomozawa et al. [2] (red circles in Fig. 1) we find

$$P = 1122.3 - 0.336\,\sigma_x \tag{3}$$

and for the case of surface-etched and annealed specimens (black circles in Fig. 1)

$$P = 1119.8 + 0.166\,\sigma_x \tag{4}$$

In order to limit the number of equations, the general formulation

$$P = P_0 + \frac{dP}{d\sigma_x}\sigma_x \tag{5}$$

with the material parameters given in Table 1 shall apply below. It is obvious from Fig. 1 that the slopes from the uniaxial tests by Tomozawa et al. [2] and from the hydrostatic pressure tests by Hemley [3] nearly disappear in the range of $P \cong 1065$-1120/cm. Especially for the data by Hemley et al. [3] it holds:

$$P = \text{const} = 1066/\text{cm} \tag{6}$$

i.e. $dP/d\sigma_x \approx 0$.

There is obviously abnormal behavior in this area, i.e. silica is very insensitive to mechanical stress in this area

### 1.2 Symmetric stretching mode (SS)

Symmetric stretching occurs at about 810/cm. A set of Raman spectra as a function of hydrostatic pressure is shown in Fig. 2 (left) as given by Hemley et al. [3].

We evaluated the peak positions and indicated the related peaks by circles. These values are shown in Fig. 2 (right) by the blue squares at stress <0.

Results evaluated from measurements by Deschamps [4] are entered as open black circles. The red squares for positive stresses are again from tensile tests by Tallant et al. [1].

It should be noted that all data in the symmetric stretching region decrease with increasing stress. The slopes are higher for tests under hydrostatic pressure than under uniaxial tests as can be seen from Table 1.

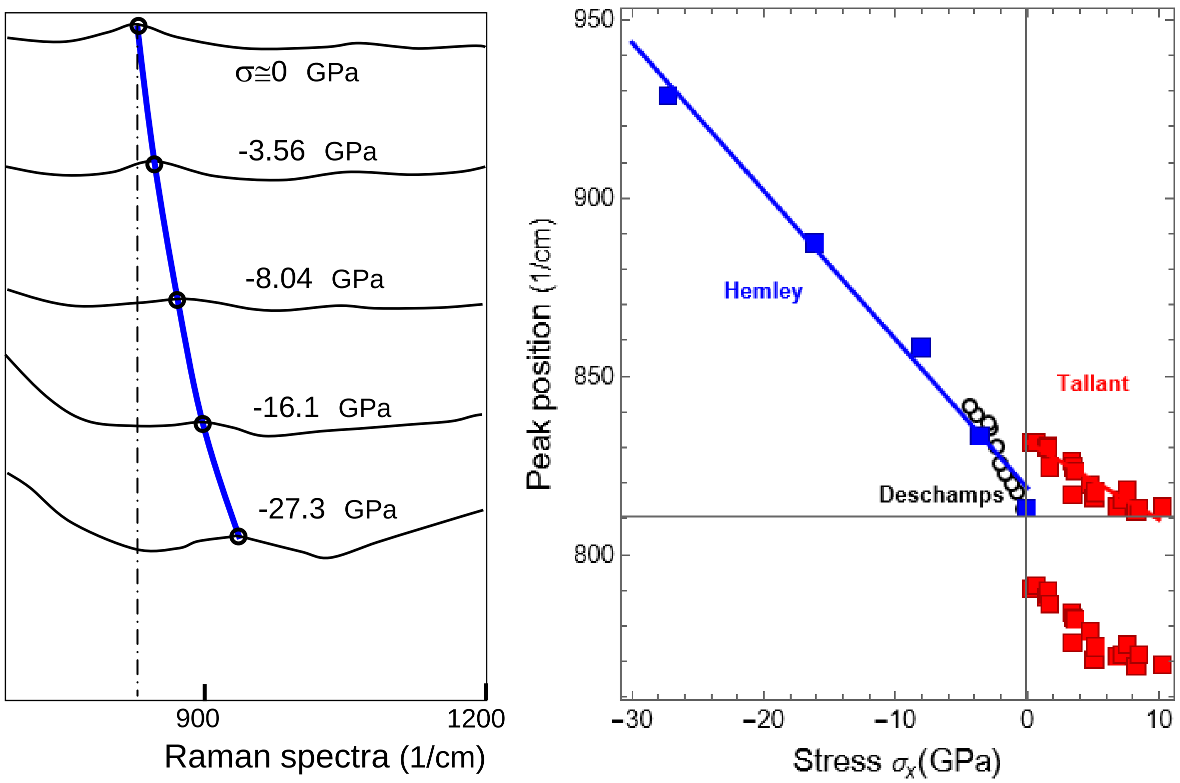


**Fig. 2** Measurements in the region of symmetric stretching (SS). Left: Measurements of Raman peak under hydrostatic stress by Hemley [3]. Right: Red squares for stress $\sigma_x$>0 from Tallant et al. [1], blue squares from Hemley [3] and black circles from Deschamps et al. [4].

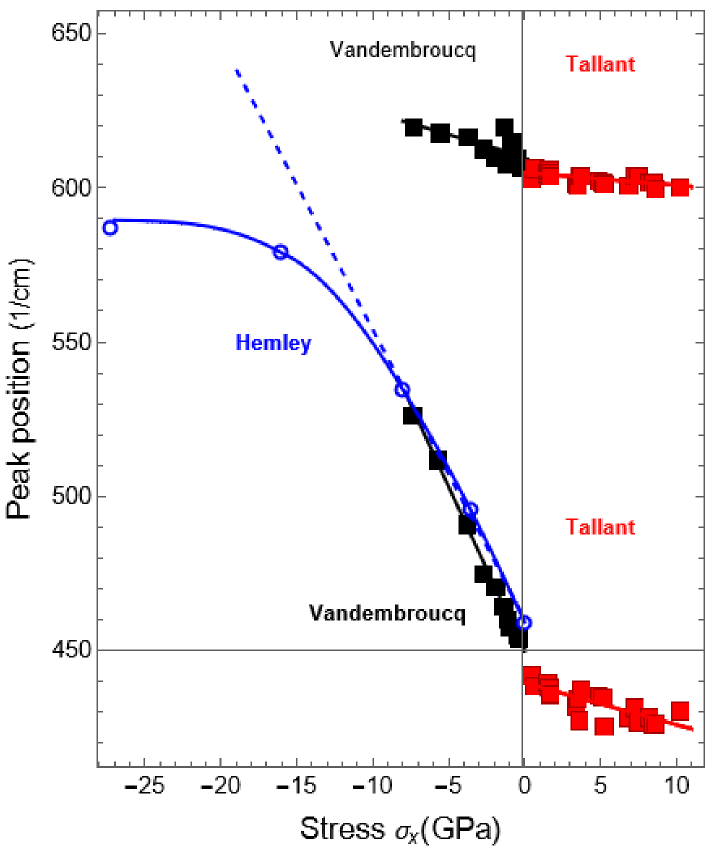


**Fig. 3** Position of Raman peaks in the region of >620/cm. Red squares for stress >0 from Tallant et al. [1], black squares: results from Vandenbroucq et al. [5], circles: data from Hemley et al [3].

### 1.3 Peak position for Raman peaks below 700/cm

Peak positions below 700/cm were studied under stresses by Tallant et al. [1], Hemley et al. [3] and Vandembroucq et al. [5]. We plot these literature results in Fig. 3. In the absence of stresses, the peak positions are at about 610/cm and 450/cm.

Figure 3 also clearly shows that the gradients under hydrostatic pressure are significantly larger than under uniaxial tensile stress.

## 2. Summary of results

In Fig. 4, all data are compiled once more. Positions in the absence of stresses and slopes from straight-line fitting are represented in Table 1.

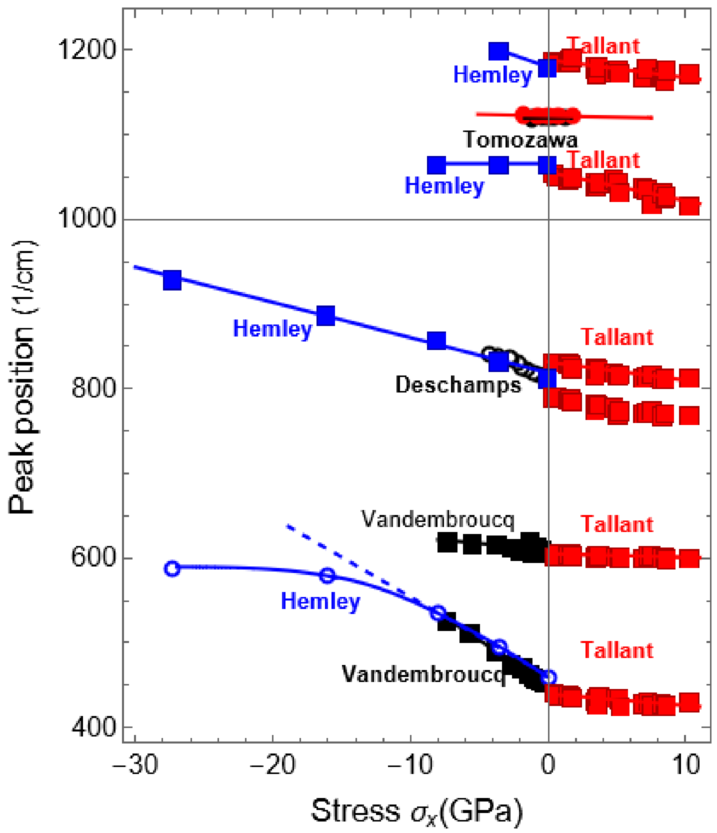


**Fig. 4** Stress-dependent peak positions as a function of the *maximum stress component* $\sigma_x$.

| Region (cm$^{-1}$) | Loading mode | $P_0$= $P(\sigma$=0) (1/cm) | d$P$/d$\sigma$ (cm$^{-1}$/GPa) | Ref. |
|---|---|---|---|---|
| 1050-1200 | uniaxial stress | 1188 | -2.11 | [1] |
| | hydrostatic | 1180 | -5.62 | [3] |
| | **uniaxial stress** | **1122.3** | **-0.336** | **[2]** |
| | **uniaxial stress** | **1119.8** | **+0.166** | **[2]** |
| | **hydrostatic** | **1066** | **0** | **[3]** |

| | | | | |
|---|---|---|---|---|
| | uniaxial stress | 1056 | -3.4 | [1] |
| ≈810 | uniaxial stress | 831 | -2.17 | [1] |
| | hydrostatic pressure | 818.7 | -4.16 | [3] |
| | hydrostatic pressure | 812 | -7.43 | [4] |
| | uniaxial stress | 791 | -2.50 | [1] |
| <650 | hydrostatic pressure | 610 | -1.45 | [5] |
| | uniaxial stress | 605 | -0.42 | [1] |
| | uniaxial stress | 490.1 | -0.514 | [1] |
| | hydrostatic pressure | 460.2 | -9.38 | [3] |
| | hydrostatic pressure | 450 | -10.6 | [5] |
| | uniaxial stress | 439.4 | -1.353 | [1] |

**Table 1:** Coefficients for peak position *P* as a function of stress under uniaxial and hydrostatic stresses according to eq.(5). Red numbers indicate anomalous behaviour.

In order to allow a direct comparison of the uniaxial measurements with the hydrostatic compression tests, we plotted the tensile data, $\sigma>0$, in terms of the hydrostatic stress $\sigma_h$. When $\sigma_x$, $\sigma_y$, $\sigma_z$ represent the stress components, the related hydrostatic stress is given as

$$\sigma_h = \frac{1}{3}(\sigma_x + \sigma_y + \sigma_z) \quad (7)$$

The results plotted vs $\sigma_h$ are compiled in Table 2. It should be noted that in case of the uniaxial test ($\sigma_y=\sigma_z=0$), the hydrostatic stress is simply $\sigma_h=\sigma_x/3$. Instead of eq.(5) we write

$$P = P_0 + \frac{dP}{d\sigma_h}\sigma_h \quad (8)$$

| Region (cm$^{-1}$) | Loading mode | $P_0 = P(\sigma_h=0)$ (1/cm) | $dP/d\sigma_h$ (cm$^{-1}$/GPa) | Ref. |
|---|---|---|---|---|
| 1050-1200 | uniaxial stress | 1188 | -6.33 | [1] |
| | hydrostatic | 1180 | -5.62 | [3] |
| | **uniaxial stress** | **1122.3** | **-1.008** | **[2]** |
| | **uniaxial stress** | **1119.8** | **+0.498** | **[2]** |
| | **hydrostatic** | **1066** | **0** | **[3]** |
| | uniaxial stress | 1056 | -10.2 | [1] |
| ≈810 | uniaxial stress | 831 | -6.51 | [1] |
| | hydrostatic pressure | 818.7 | -4.16 | [3] |
| | hydrostatic pressure | 812 | -7.43 | [4] |

| | | | | |
|---|---|---|---|---|
| | uniaxial stress | 791 | -7.50 | [1] |
| <650 | hydrostatic pressure | 610 | -1.45 | [5] |
| | uniaxial stress | 605 | -1.26 | [1] |
| | uniaxial stress | 490.1 | -1.54 | [1] |
| | hydrostatic pressure | 460.2 | -9.38 | [3] |
| | hydrostatic pressure | 450 | -10.6 | [5] |
| | uniaxial stress | 439.4 | -4.06 | [1] |

**Table 2:** Coefficients for peak position $P$ for hydrostatic stresses $\sigma_h$ according to eq.(7). Red numbers again indicate an anomalous behaviour.

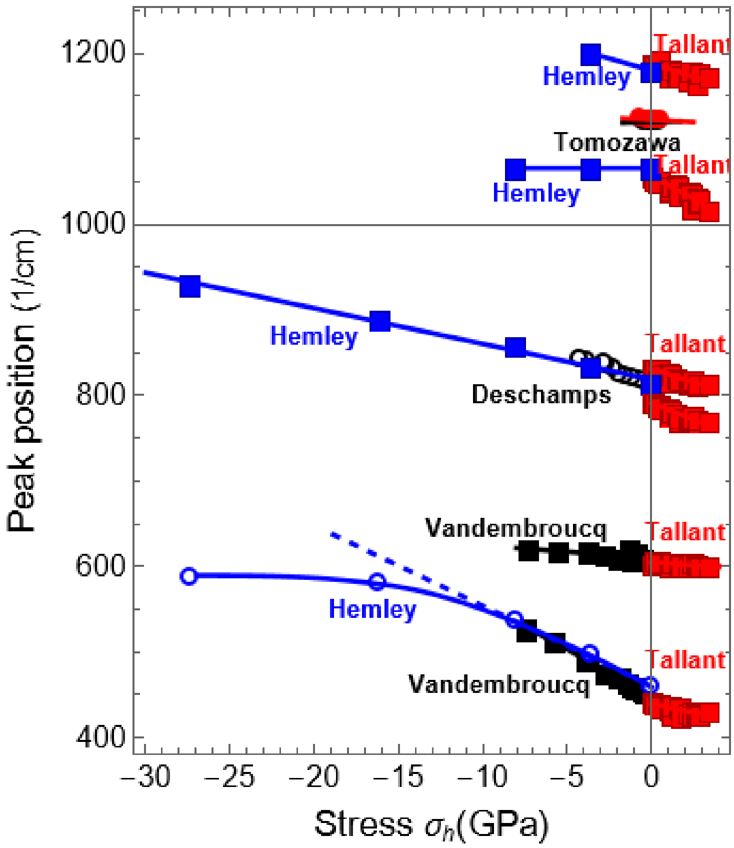


**Fig. 5** Stress-dependent peak positions as a function of the *hydrostatic stress* $\sigma_h$.

## 3. Main conclusions:

- In the wave number region <1000/cm, all studies show decreasing peak positions with increasing stresses.
- When the change of the peak position is plotted against the *maximum stress* component, the slopes of the decreasing straight lines are significantly steeper in compression than in tension.

- When the peak positions are plotted against the *hydrostatic stress*, the slopes of the lines become quite comparable.
- Of particular interest is the behavior in the asymmetric stretching mode (AS). In the range from about 1065/cm to 1120/cm, the influence of stress in both the tensile and compressive ranges is almost negligible. The results by Tomozawa et al. [2] are confirmed by the evaluation of the Raman spectra according to Hemsley et al. [3]. The reason for the abnormal behavior will be investigated in a separate study.

## References


1 Tallant DR, Michalske TA, Smith WL. J. Non-Cryst Solids **106**(1988): 380-82
2 Tomozawa M, Lee YK, Peng YL, J. Non-Cryst Solids **242**(1998), 104-109.
3 Hemley R.J., Mao K.H., Bell P.M., Myssen B.O., Physical Review Letters, **57**(1986), 747-750.
4 Deschamps T, Martinet C, de Ligny D, Champagnon B, J. Non-Cryst Solids **355**(2009), 1095-1098.
5 Vandembroucq D, Deschamps T, Coussa C, Perriot A, Barthel, Champagnon B, Martinet C, HAL 2008, hal-00258599v1.

KIT Scientific Working Papers
ISSN 2194-1629
www.kit.edu